A Dissemination Model Based on Psychological Theories in Complex Social Networks

Tianyi Luo, Zhidong Cao, Daniel Zeng, *Fellow, IEEE*, and Qingpeng Zhang, *Member, IEEE*

Abstract—Information spread on social media has been extensively studied through both model-driven theoretical research and data-driven case studies. Recent empirical studies have analyzed the differences and complexity of information dissemination, but theoretical explanations of its characteristics from a modeling perspective are underresearched. To capture the complex patterns of the information dissemination mechanism, we propose a resistant linear threshold (RLT) dissemination model based on psychological theories and empirical findings. In this article, we validate the RLT model on three types of networks and then quantify and compare the dissemination characteristics of the simulation results with those from the empirical results. In addition, we examine the factors affecting dissemination. Finally, we perform two case studies of the 2019 novel Corona Virus Disease (COVID-19)-related information dissemination. The dissemination characteristics derived by the simulations are consistent with the empirical research. These results demonstrate that the RLT model is able to capture the patterns of information dissemination on social media and thus provide model-driven insights into the interpretation of public opinion, rumor control, and marketing strategies on social media.

Index Terms—Complex networks, differential dissemination, dissemination mechanism, information dissemination, psychology.

I. Introduction

CURRENTLY, with the rapid progress of online social media, a large amount of information is flooding into and changing people's lives [1], [2]. In the presidential race between Trump and Clinton in 2016, social media, represented by Facebook, became the main battlefield of public opinion, and various kinds of news were mixed and widely spread [3]–[5]. The immeasurable invisible force of social media also had an essential impact on Britain's exit from the EU [6]–[8]. The public believes that human society has entered a *post-fact* era [9], in which the mainstream media has lost its absolute advantages in the opinion market. People's opinions are becoming more easily affected by emotions and personal beliefs. Rumors and excessive emotions are gradually shaping individuals' inner spiritual world and having an irreversible impact on societal development. Thus, research on the laws and mechanisms of information dissemination in the *post-fact* era has both theoretical value and practical significance.

To analyze the spread and cessation of online information, including rumors, public opinion, and news, transmission processes are often treated as mathematical models. In general, information dissemination models in social networks can be divided into three categories: 1) linear threshold (LT) models [10]–[12]; 2) independent cascade (IC) models [13], [14]; and 3) infectious disease models [15], [16]. Because the information dissemination process in social media is similar to the outbreak of epidemics, infectious disease models are often used to model online information dissemination. Zanette [17], [18] first applied the infectious disease model SIR to study rumor propagation in static and dynamic small-world networks. Nekovee *et al.* [19] concluded that scale-free social networks are prone to spreading rumors. Pan *et al.* [20] studied the propagation behavior of rumors on scale-free networks with a power-law distribution and variable clustering coefficients. Later scholars [21]–[23] found that SIS and SIR models were insufficient to describe the process of information dissemination on the Internet, and so models considering psychological factors were proposed. Considering the hesitation mechanism, some scholars have proposed an improved SEIR model [24], [25]. Taking into account the memory and forgetting mechanism, Zhao *et al.* [26], [27] proposed the SIHR model. Xiao *et al.* [28] and [29], and Li *et al.* [30] combined evolutionary games with the traditional SIR epidemic model to reflect the confrontation and symbiosis of rumor and anti-rumor information. Based on evolutionary games, Xiao *et al.* [31] also considered the diversity and complexity of the feature space of rumor spreading and made full use of the advantages of representation learning in data feature extraction. As the mainstream graph-based information diffusion model, the LT and IC models have been continuously improved and developed in research. He *et al.* [32] extended the classical LT model and studied the propagation of competitive influences in social networks under the competitive LT (CLT) model. Saito *et al.* [33] considered the time delay

Tianyi Luo is with the State Key Laboratory of Management and Control for Complex Systems, Institute of Automation, Chinese Academy of Sciences, Beijing 100190, China, and also with the School of Artificial Intelligence, University of Chinese Academy of Science, Beijing 100049, China (e-mail: luotianyi2017@ia.ac.cn).

Zhidong Cao and Daniel Zeng are with the State Key Laboratory of Management and Control for Complex Systems, Institute of Automation, Chinese Academy of Sciences, Beijing 100190, China (e-mail: zhidong. cao@ia.ac.cn; dajun.zeng@ia.ac.cn).

Qingpeng Zhang is with the School of Data Science, City University of Hong Kong, Hong Kong (e-mail: qingpeng.zhang@cityu.edu.hk).

of propagation and proposed the continuous-time delay LT (CTLT). Yang *et al.* [34] proposed a threshold model with one-direction state transition (LT1DT) for modeling two different types of competitive information propagation in the same network. The continuous-time IC (CTIC) is a continuous-time version of the IC model that considers both interpersonal influence and diffusion delay patterns [35].

In addition to researching information dissemination based on model-driven and simulation networks, with the development of Facebook, Twitter, and other social platforms, many empirical works have analyzed news propagation characteristics [36]–[40]. In 2018, Vosoughi *et al.* [41] published a systematic study of information dissemination in *Science* that quantitatively analyzed the diffusion characteristics of 126 000 information cascades distributed on Twitter; the results confirmed that the news has high diffusion specificity and complexity on social networks. The dynamic characteristics of differential diffusion have aroused widespread concern and have been applied to many studies. However, a theoretical explanation of the complex propagation phenomenon from a model perspective is still lacking. To explain the complex differential propagation phenomenon and better understand the diffusion mechanism, we propose a novel information dissemination model based on cognitive psychology.

Unlike viruses, diseases, and knowledge transmission, the diffusion of information, especially rumor and public opinion, is a multidimensional process driven mainly by psychological elements [42]. Online information propagation is closely related to personal psychological qualities. People forward and disseminate online information due to interest and attention. Combining attenuation theory and interference theory, after people obtain information, time passes and new news is generated; the previous news will be disturbed by the new information, and its intensity will continue to decay. People also pay less attention and devote less interest to the previous news, and the intensity of the previous information is weakened by the entry of new information. In addition to these theoretical studies, we have also found evidence in relevant empirical studies. In [41], as the cascade depth increases, it becomes more difficult for online information to spread. Inspired by psychological theories and informed by our knowledge of spread characteristics, we apply the attention attenuation theory and interference theory from psychology to our dissemination model.

Thus, in this article, we propose a novel information dissemination model based on attention attenuation theory and interference theory, namely, the resistant LT (RLT) model. We verify the propagation dynamics behavior of the RLT model on three types of synthetic networks: 1) the small-world networks; 2) the scale-free networks; and 3) the random networks. We then quantify and compare the four types of propagation characteristics from the simulation results with the empirical results [41]. In addition, to understand the relevant factors that affect news dissemination on social platforms, we conduct a sensitivity analysis and explore the influence of the network structure and the model's parameters on information dissemination. These factors have different practical meanings in different scenarios. Finally, we address the case studies to

demonstrate the effectiveness and applications of the proposed model, using the RLT model to simulate the spread of online public opinion and news related to the Corona Virus Disease 2019 (COVID-19) pandemic. The simulation results, in shape, are largely consistent with the statistical characteristics of rumor diffusion [41]. The results show that the RLT model can describe the process of differential diffusion and interpret public opinion of COVID-19 outbreak laws. We also find that real social networks are closer to a mixture of small-world and scale-free networks. The results provide a reference for effective marketing, public opinion guidance, and the control of rumors in social media.

The contribution of this article is fourfold. First, we propose a novel model considering attention attenuation theory and interference theory from psychology. The model can explain the empirical complex dissemination phenomena and interpret the outbreak laws and internal mechanisms of the development of public opinion about COVID-19. Second, by using the proposed model simulation on three types of networks, we find that some statistical propagation characteristics of real social networks are closer to a mixture of small-world and scale-free networks, leading us to speculate that real social networks are a mixture of these two types. Third, we explore the effect of network structure and model parameters on information dissemination. We find that the most efficient spread of news occurs in scale-free networks and that small-world networks slow down and draw out the spreading process. The effect of the initial threshold on transmission uncertainty is evident in scale-free networks. Finally, we apply the experimental conclusions to different actual scenarios and provide suggestions for controlling false news and strategies for delivering information.

The remainder of this article is organized as follows. In Section II, the information propagation model based on psychology is introduced, and both the simulation and the sensitivity analysis are carried out. Section III presents our simulation findings. Section IV addresses two case studies to demonstrate the effectiveness of the proposed model. Finally, Section V draws conclusions and provides directions for future research.

II. MODEL CONSTRUCTION AND SIMULATION

A. Model

1) Psychological Theory: It includes attention attenuation theory and interference theory.

Attention Attenuation Theory: When information passes through the attenuator, critical information both passes through and is reflected in the consciousness of the person, while the intensity of any information that is not given attention is weakened.

Interference Theory: Forgetting in short-term memory is caused when other information interferes with the information stored in short-term memory.

These two theories also correspond to the psychological effects mentioned in [35]: for a large number of infective individuals, the infection force will decrease as the number of infective individuals increases because, in the presence of a

large number of infective individuals, the population will tend to reduce the number of contacts per unit time. In addition to these theoretical studies, we have also found evidence in the relevant empirical studies. In Vosoughi *et al.*'s study [41], as the cascade depth increases, the spread of online information becomes more difficult.

We apply the attention attenuation theory and interference theory to information transmission. People forward and disseminate online information based on interest and attention. According to the attention attenuation theory, after people obtain information, over time, the attention they give to that information will gradually decrease and shift. At the same time, we consider the interference theory. With the continuous production of novel news, the previous news will be disturbed by various pieces of new information. The intensity of the previous information will be weakened by the entry of new information, and people will pay less attention to and have less interest in the previous news. Therefore, the early stage of news production has the most significant impact on the public. With the passage of time, users' attention is constantly attenuated and disturbed by all kinds of new information. As a result, users become immune to prior information, their resistance to information becomes increasingly stronger, and the spread of information in the network becomes increasingly difficult.

2) RLT Model: The RLT model is an extension of the LT model. The basic idea of the LT model is to capture the phenomenon in which users are affected by the behavior of those around them and thus participate in the activity. In the context of information dissemination, this behavior refers to the user forwarding a particular news item. In the LT model, each node has an activation threshold, which indicates how easily that node is affected. A node in an inactive state will be activated only when the sum of the influence of its active neighbor nodes is greater than or equal to its threshold. In the information dissemination model, the active state means that the node forwards the information.

In the classical LT model, the activation threshold does not change with time (cascade depth), meaning that it is constant. This would mean that users' attention and interest in an item of online information remain unchanged in the information dissemination scenario, which is contradictory to the psychological mechanism. To address this concern, considering the attention attenuation theory and interference theory, we propose the RLT model. In the RLT model, resistance means that people's attention and interest in social network information diminish, and the activation threshold parameter is used to represent this resistance. When the user's interest and attention to information decrease, the behavior of forwarding information will be resisted and become more difficult (that is, the activation threshold will become higher). The activation threshold of nodes grows nonlinearly over time (cascade depth) and eventually converges to a maximum value of 1. The nonlinear growth function can be personalized based on the information dissemination scenario. In our work, the change in threshold conforms to the law of the logistic growth model.

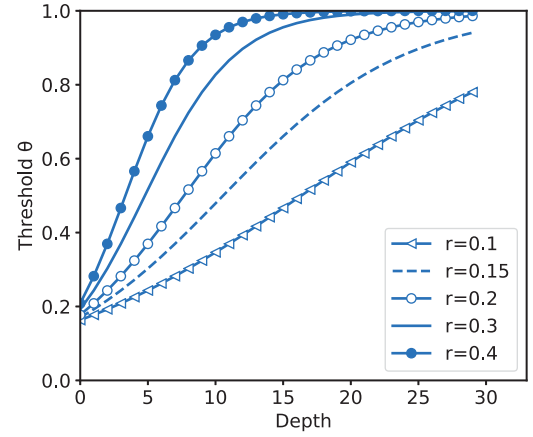In this section, we formally describe the RLT model in detail.

Fig. 1.   Activation threshold of the RLT model changes with propagation depth at different growth rates *r*.

The social network is mathematically formalized as a directed graph G, and each node v_i in G has two states f (active state 1 and inactive state 0).

Each node v_i has an activation threshold θ_{v_i}. For each node v_i, the sum of the influence weight generated by all neighbors cannot exceed 1

$$\sum_{w \in N(v_i)} b_{w,vi} \leq 1 \tag{1}$$

where

$$b_{w,v_i} = 1/\text{in\_deg}(v_i) \tag{2}$$

where $\text{in\_deg}(v_i)$ is the in-degree of node v_i. $N(v_i)$ is the neighbor node of node v_i, and b_{w,v_i} is the influence weight of node w on node v_i. In this model, we set all nodes v_i to have the same threshold θ at the same time.

At time t, v_i will be activated when the sum of the weights of the activated neighbors exceeds its threshold

$$\sum_{w \in N(v_i), w \text{ is active}} b_{w,v_i} \geq \theta_{v_i}. \tag{3}$$

At time $t + 1$, v_i is in activated state 1 and has an impact on its inactive neighbor node. The propagation ends when no more nodes can be activated.

When the information propagates to depth $i(i > 0)$, the activation threshold $\theta(i)$ of the $i+1$ layer is an increasing function of i and the growth law conforms to the logistic growth model

$$\frac{d(\theta)}{di} = \frac{r \cdot \theta \cdot (k - \theta)}{k} = r \cdot \theta \cdot (1 - \frac{\theta}{k}) \tag{4}$$

$$\theta(i) = \frac{k \cdot \theta(0) \cdot e^{ri}}{k + \theta(0) \cdot (e^{ri} - 1)} \tag{5}$$

$$\lim_{i \to \infty} \theta(i) = k \tag{6}$$

where r is the logistic growth rate. Since the activation threshold does not exceed 1, the parameter $k = 1$. Fig. 1 is the S-shaped curve showing how the activation threshold $\theta(i)$ varies with the propagation depth at different growth rates r.

In our simulation, we use nodes in the network to represent users in various states. Active state 1 refers to users who are affected by the information and have the ability to

disseminate that information. Active state 0 refers to users who have not received the information or who have received information but are not affected by it and unable to spread it. The corresponding transformation process is as follows.

Step 1: Select a network G, for each node in G, initialize the activation threshold $\theta(0)$, and set the growth rate r of the RLT model.

Step 2: In network G, select a node $v_i (i \in V_G)$ completely randomly and with equal probability to be the initial node for information transmission in the simulation network at initial time t_0.

Step 3: According to the RLT model rule, the simulation computing is started in G, and it can be found that at time t_1, some neighboring nodes $N(v_i)$ of the initial node v_i are activated. Activation rule: if $\sum_{w \in N(v_i), w \text{ is active}} b_{w,v} \geq \theta_{v_i}$, v_i is activated.

Step 4: At t_2, the nodes activated at t_1 influence their neighboring nodes. Within each time step, the spreader disseminates the news to its neighbors. The above process is repeated. The propagation ends when no more nodes can be activated.

The propagation time is represented by the depth of propagation.

B. Model Simulation

1) Network Generation: A real social media network is a complex system that generally contains various network features. To thoroughly study the propagation characteristics of information on social platforms, we choose three types of networks for simulation, namely, small-world networks, scale-free networks, and Erdős–Rényi random networks. The characteristics of the five networks in the simulation are shown in Table I.

The WS small-world model proposed by Watts and Strogatz [43] is used to construct networks G_1 and G_2. The WS small-world network was constituted by randomly rewiring the connected edges in the rule network. By adjusting the random rewiring probability, the regular network will transition to a random network. The clustering coefficient of the small-world network is large and will decrease significantly only when the rewiring probability is relatively large. The random rewiring probabilities of small-world networks G_1 and G_2 are 0.8 and 0.2, respectively.

Barabási and Albert [44] proposed a scale-free network model (referred to as the BA model). The node degree of the network follows a power-law distribution and has scale-free properties. The scale-free network G_3 is generated using the BA growth network model. During the generation process, new nodes tend to connect with nodes with higher connectivity.

The WS model and BA model are two representative network generative models, but each lacks the property of the other: the WS model shows high clustering but without the power-law degree distribution, while the BA model with its scale-free nature does not possess high clustering. Holme and Kim [45] proposed a network model that has both a perfect power-law degree distribution and high clustering. This model also considers that social networks typically show local transitivity: if a person A knows B and C, then B and C are likely to know each other. Compared with the BA model, the
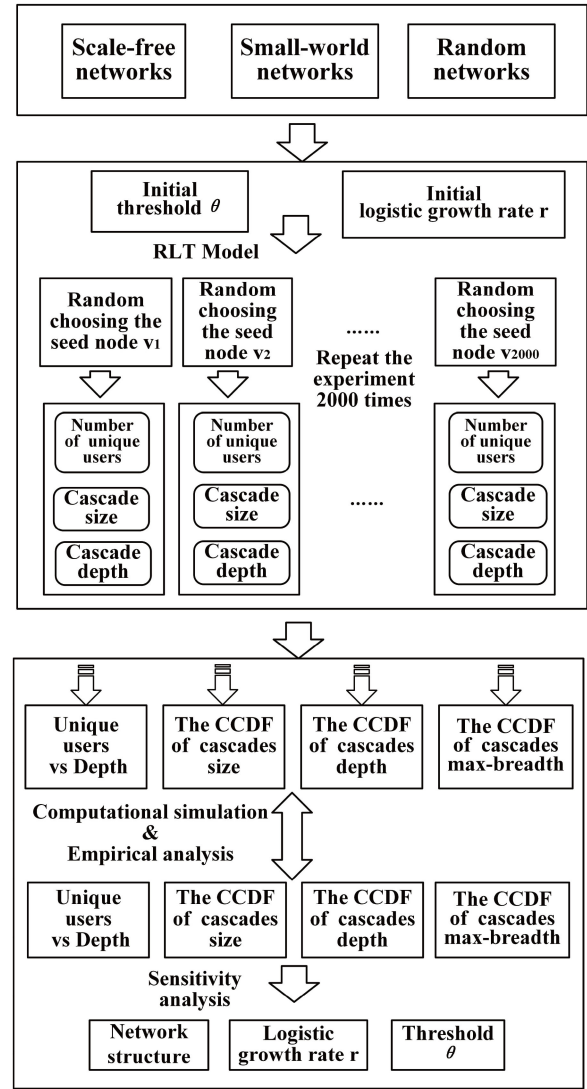

Fig. 2. Analysis framework of the computational simulation.

probability of adding a triangle after adding random edges will increase during the generation process. The scale-free network G_4 was constructed using this model. The scale-free network G_3 has a low average network clustering coefficient, and the improved scale-free network G_4 has small-world characteristics.

Finally, the Erdős–Rényi model proposed by Erdős and Rényi [46] was used to generate a random network G_5. In the random network, node degrees follow a Poisson distribution, and most nodes have roughly the same number of connections (nearly average degree). The average path length is proportional to the logarithm of the network size. The clustering coefficient of G_5 is minimal, indicating that the network nodes are distributed more evenly, and the degree of node aggregation is very low.

2) Model Simulation and Statistics: In this article, the Monte Carlo method was used to conduct simulation experiments to verify whether our model can reproduce the research findings of Soroush based on empirical data, with the aim of adequately expressing the driving mechanism behind the

TABLE I
CHARACTERISTICS OF THE FIVE NETWORKS IN THE SIMULATION

Network	Node	Edge	Average shortest path length	Average clustering coefficient
Small-world network G_1	10,000	30,000	5.47	0.005
Small-world network G_2	10,000	30,000	6.95	0.313
Scale-free network G_3	10,000	29,991	4.27	0.006
Scale-free network G_4	10,000	29,991	4.26	0.27
Random network G_5	10,000	29,991	5.34	0.0005

complex propagation phenomenon. Fig. 2 shows the computational simulation analysis framework.

We conduct the propagation simulation based on the RLT model. First, we record and calculate the value of the propagation experiment in the complete process of each propagation: the number of people per layer, the size of the cascade, the depth of the cascade, and the max-breadth of the cascade. By repeating this 2000 times, the values of the propagation under 2000 completely random experiments can be obtained.

The concepts involved in the propagation of experimental procedures and results are defined as follows [41].

1) *News and Rumor:* We define news as any story or claim with an assertion in it and a rumor as the social phenomena of a news story or claim spreading or diffusing through the network.

2) *Cascade:* In rumor propagation, a complete forwarding chain with a common single origin is called a cascade (Fig. 3 is a sample cascade).

3) *Size/Unique Users:* The size of a rumor cascade corresponds to the number of unique users in that cascade. Users can only transmit information once in the network. The cascade size indicates the number of users infected by this rumor source in one propagation. Fig. 3 shows the size of the sample cascade at different depths; and the size of the full cascade is 11.

4) *Depth:* The depth of a node is the number of edges from the focal node to the initial node. The depth of a rumor cascade is the maximum depth of the nodes in the cascade, which represents the maximum number of forwarding layers from the source of the rumor. Fig. 3 shows the depth measurement for our sample cascade, which in this case is 3.

5) *Max-Breadth:* At each depth, the breadth of a cascade is the number of nodes at that depth. The maximum breadth of a rumor cascade is its maximum width and represents the maximum number of propagations of the message in the number of unit steps, which can be defined as

$$B = \max(bi), \quad 0 \leq i \leq d \tag{7}$$

where d denotes the cascade depth, and b_i denotes the breadth of a cascade at depth i. Fig. 3 shows the breadth of the sample cascade at each depth. The max-breadth of this cascade is 5.

According to the simulated values for the 2000 propagations (each propagation experiment can be regarded as one sample), the statistical characteristics of the propagation process of the population composed of 2000 samples can be
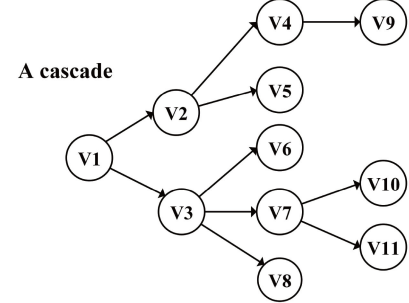
Fig. 3. Size, depth, and breadth calculated for sample rumor cascade.

analyzed as follows: the relationship between the depth of transmission and the average number of people transmitted is analyzed and complementary cumulative distribution functions (CCDFs) are constructed of cascade size, depth, and max-breadth, where the CCDF represents the sum of the occurrence probability of all values greater than a for a continuous function

$$F(a) = P(x > a). \tag{8}$$

3) Sensitivity Analysis: The evolutionary process of information dissemination is affected by many complex factors. The sensitivity analysis of the model is divided into three parts: 1) the influence of the network structure; 2) the model parameter growth rate r; and 3) the initial threshold $\theta(0)$ of the model.

The specific parameters for the sensitivity analysis of the model are set as follows.

1) Maintain $\theta(0) = 0.15$ and $r = 0.15$, and performing experiments in five networks: G_1, G_2, G_3, G_4, and G_5.

2) Maintain $\theta(0) = 0.15$, in the case of $r = 0.1, 0.15, 0.2$, performing experiments in five networks: G_1, G_2, G_3, G_4, and G_5.

3) Maintain $r = 0.15$, in the case of $\theta(0) = 0.05, 0.15, 0.3$, performing experiments in three networks: G_1, G_3, and G_5.

III. RESULTS

Fig. 4 shows the statistics for the two thousand simulation results of the RLT model on five simulated networks under
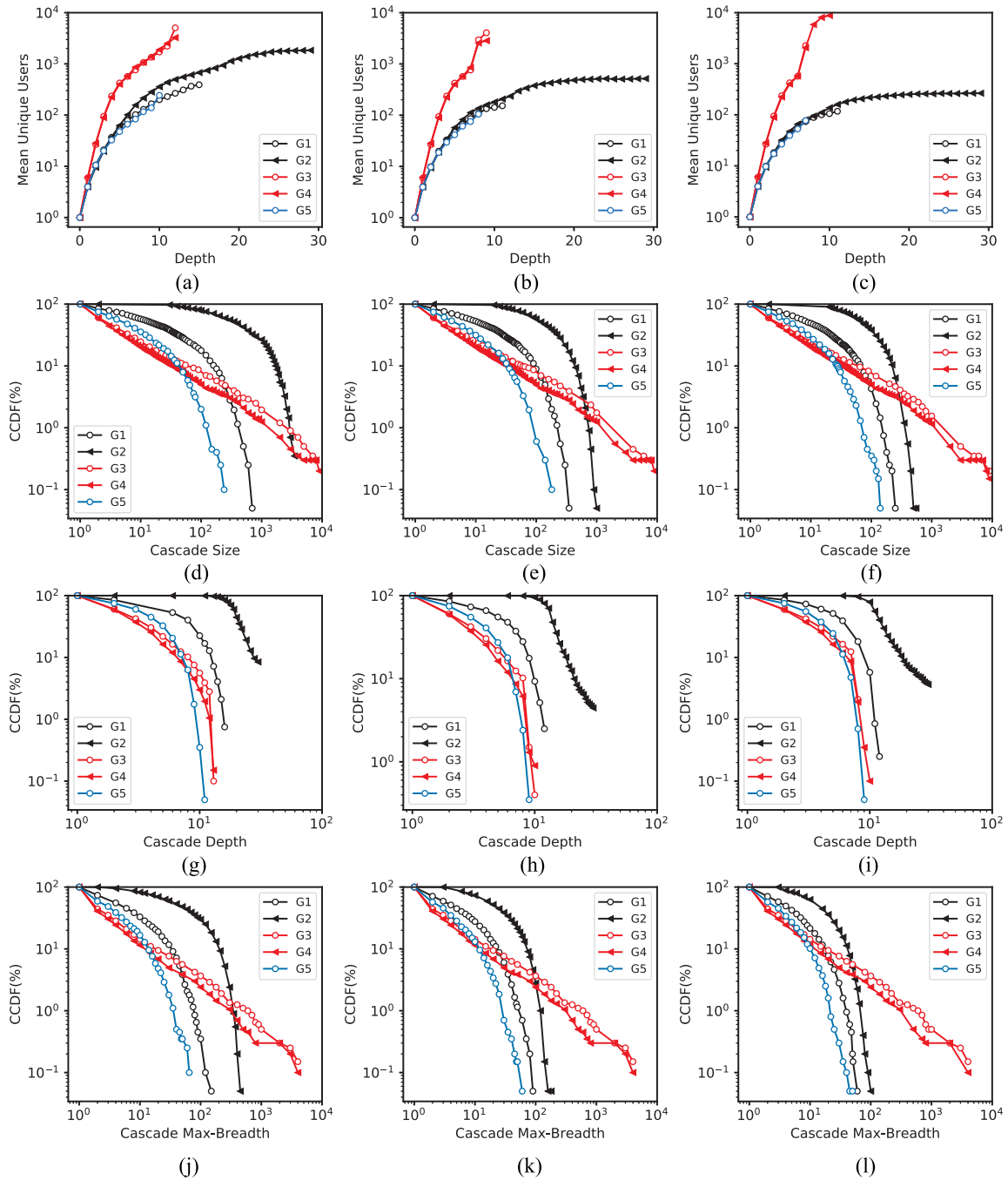
Fig. 4. Statistics of the simulation results of the RLT model on five simulated networks (G_1 and G_2 are small-world networks, black line; G_3 and G_4 are scale-free networks, red line; and G_5 is random network, blue line) under specific conditions ($\theta(0) = 0.15$, $r = 0.1, 0.15, 0.2$). (a)–(c) show the relationship between the number of mean unique users in 2000 experiments and propagation depth when growth rate $r = 0.1, 0.15, 0.2$. (d)–(f) show the CCDFs of rumor cascade sizes when $r = 0.1, 0.15, 0.2$. (g)–(i) show the CCDFs of rumor cascade depths when $r = 0.1, 0.15, 0.2$. (j)–(l) show the CCDFs of rumor cascade max-breadths when $r = 0.1, 0.15, 0.2$.

specific conditions. Fig. 5 shows the statistics for the results of 2000 simulations on three simulated networks under the different initial thresholds.

A. Comparison of Simulation Results With Empirical Results

Vosoughi *et al.*'s [41] statistical research based on empirical data shows that truth rarely spreads to more than 1000 people whereas the top of 1% false-news cascades is routinely diffused between 1000 and 100 000 people. G_1 in Fig. 4(a) can

represent this truth dissemination characteristic. It can be seen from Fig. 4(a) and (d) that the maximum cascade size on G_3 and G_4 is close to the total user number 10 000, the top of 0.2% of cascade size can nearly reach this value, and the top of 1 % of cascade is routinely diffused between 2000 and 10 000 people. These characteristics are roughly consistent with the propagation characteristics of false news. Vosoughi *et al.*'s [41] research also shows that the depth of true news propagation rarely exceeds ten layers, and the features of G_1, G_3, G_4,

TABLE II
RESULTS OF SIMULATION WITH INITIAL CONDITIONS OF $\theta(0) = 0.15$, $r = 0.15$

$\theta(0) = 0.15$, $r = 0.15$	Maximum cascade size	Average cascade size	Maximum cascade depth	Maximum cascade max-breadth
Small-world network G_1	383	153	12	90
Small-world network G_2	1,081	517	30	187
Scale-free network G_3	9,997	4,059	10	4,764
Scale-free network G_4	9,997	2,847	10	5,041
Random network G_5	186	105	9	62

and G_5 in Fig. 4(g)–(i) are consistent with this conclusion. Comparing G_1 and G_3 curves in Fig. 4(d) and (e), we can find that the empirical data's CCDF curve form for the cascade size is between those of the small-world and scale-free networks, which shows that the news propagation characteristics of real social networks are closer to a mixture of small-world and scale-free networks.

B. Influence of Network Structure on Information Dissemination

For ease of explanation, the following results are analyzed with the initial conditions of $\theta(0) = 0.15$ and $r = 0.15$, and the comparison under different r is shown in the next section. We extracted some important feature values from Fig. 4(b), (e), (h), and (k) listed in Table II.

Cascade Size: Table II shows that both the maximum cascade size and average cascade size of the propagation are the largest in a scale-free network. They are much smaller in small-world and random networks. Table II shows that the aggregation of small-world networks has a significant impact on the scale of transmission. As the aggregation increases, the maximum cascade size that the small-world networks can achieve will increase significantly, as will the probability of occurrence of large values. The aggregation of scale-free networks has a relatively small impact on the maximum cascade size.

Cascade Depth: Fig. 4(b) and (h) and Table II show that information has the highest potential for reaching the maximum depth of transmission in small-world networks. Highly clustered G_2 can be transmitted to 30 layers, far exceeding the number in scale-free networks and random networks: the cascade depth of scale-free networks rarely exceeds ten layers. The random network G_5 has the smallest potential for maximum propagation depth. The aggregation of small-world networks has a significant impact on the maximum cascade depth. As the aggregation increases, the maximum cascade depth that small-world networks can achieve will increase significantly, and the probability of occurrence of large values will also rise dramatically. The aggregation of scale-free networks has a weak influence on the maximum cascade depth.

Cascade Max-Breadth: Fig. 4(k) and Table II show that the maximum cascade max-breadth of a single transmission in a scale-free network is the largest. The aggregation of small-world networks has a significant impact on the maximum cascade max-breadth; and the aggregation of scale-free networks has a weak influence on the maximum cascade max-breadth.

C. Influence of Model Parameter r on Information Dissemination

When $r = 0.1, 0.15, 0.2$, the overall conclusion of Section III-B remains valid (Fig. 4), with some local effects, as follows.

Small-World Networks: As seen from the G_1 and G_2 curves in Fig. 4, with the increase in r, the propagation in small-world networks is significantly inhibited. The cascade depth, cascade size, and cascade max-breadth are reduced. When the growth rate r increases from 0.1 to 0.2, the average spread scale is reduced from 391 to 117 in G_1 and reduced from 1842 to 265 in G_2. The scale of spread is reduced by 70% and 86%, respectively, [Fig. 4(a)–(c)]. The CCDF curve for the cascade size on G_1 and G_2 overall shifts right [Fig. 4(d)–(f)], and the scale of transmission is reduced. In particular, when the growth rate r increases from 0.1 to 0.15, the proportion of transmissions with a cascade size of more than 1000 decreased from 26.6% to 0.05% in G_2. The maximum cascade depth of G_1 was reduced from 16 to 12 [Fig. 4(g)–(i)]. When $r = 0.1$, 12.9% of the propagation cascade depth exceeds 12 in G_1. The cascades of max-breadth decrease with increasing r in the small-world networks [Fig. 4(j)–(l)].

Scale-Free Networks: As seen from the G_3 and G_4 curves in Fig. 4, with the increase in r, the propagation in the scale-free networks has been relatively little affected. When the growth rate r increases from 0.1 to 0.2, in the scale-free network G_3 and G_4, the propagation scale of the first seven layers remains unchanged. After seven layers, the number of users mutates, and the transmission was suppressed and stopped quickly [Fig. 4(a)–(c)]. When the growth rate r increased from 0.1 to 0.2, the proportion of transmissions with a cascade size of more than 1000 decreased from 1.95% to 1.55%, and the proportion of transmissions with a cascade size of more than 5000 decreased from 0.5% to 0.35% in G_3. The maximum depth is reduced as r increases; and the maximum cascade depth of G_3 was reduced from 13 to 8 [Fig. 4(d)–(f)].

Random Networks: As seen from the G_5 curve in Fig. 4, with the increase in r, the propagation in the random network G_5 is somewhat inhibited: when r increased from 0.1 to 0.2, the average cascade size decreased from 243 to 77 [Fig. 4(d)–(f)], and the overall spread depth decreased [Fig. 4(g)–(i)]. The cascade max-breadth of G_5 is almost unaffected by r [Fig. 4(j)–(l)].

D. Influence of Initial Threshold $\theta(0)$ on Information Dissemination

Small-World Networks: According to Fig. 5(a), (d), (g), and (j), the entire propagation process is uniformly suppressed due
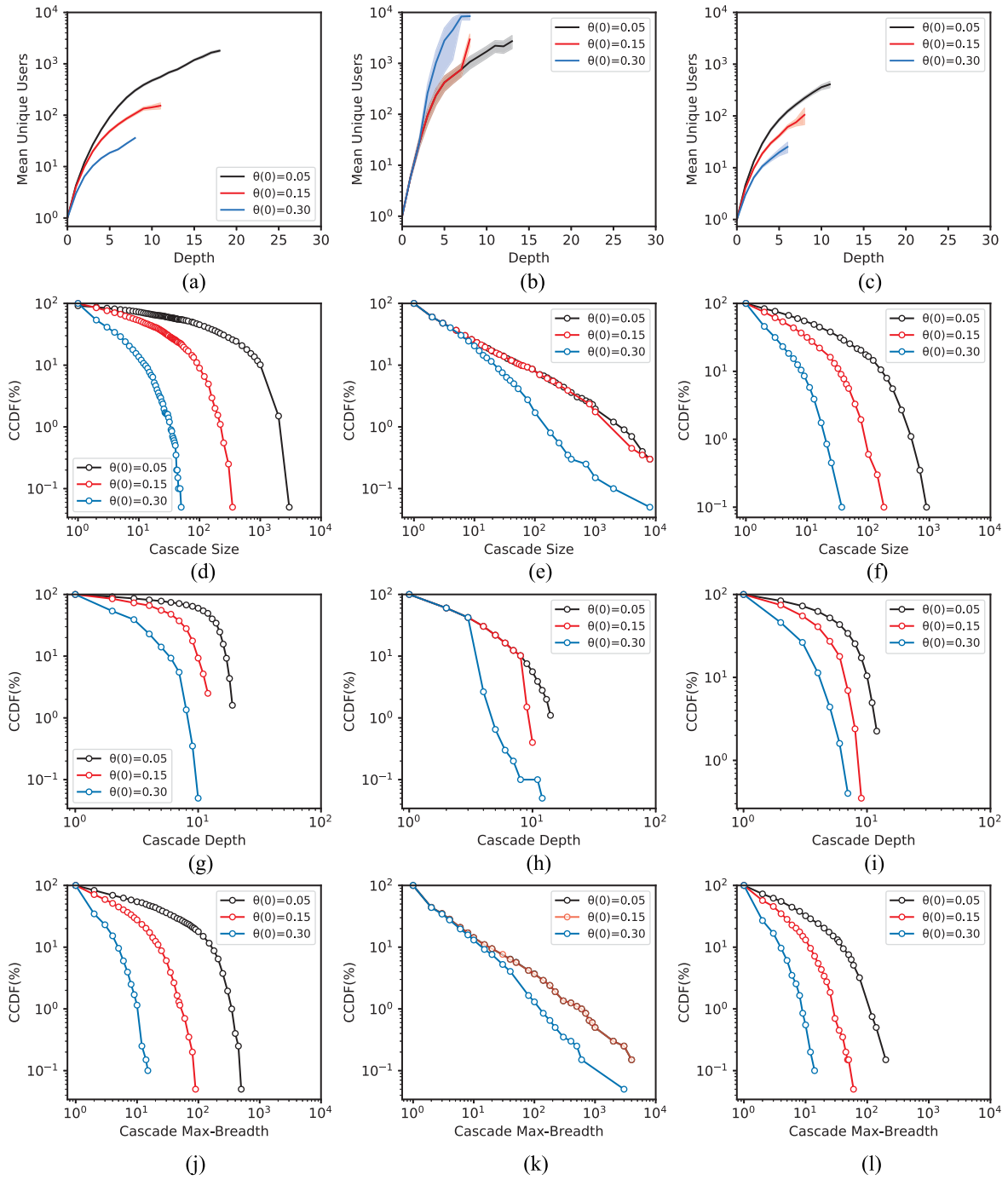
Fig. 5.   Statistics of the simulation results of the RLT model on three simulated networks (G_1 is a small-world network; G_3 is a scale-free network; and G_5 is a random network) under specific conditions ($\theta(0) = 0.05(black\ line)$, $0.15(red\ line)$, $0.30(blue\ line)$). (a)–(c) show the relationship between the number of mean unique users in 2000 experiments and propagation depths on G_1, G_3, and G_5. (d)–(f) show the CCDFs of rumor cascade sizes on G_1, G_3, and G_5. (g)–(i) show the CCDFs of rumor cascade depths on G_1, G_3, and G_5. (j)–(l) show the CCDFs of rumor cascade max-breadths on G_1, G_3, and G_5.

to the increase in the initial threshold: cascade size, cascade depth, and cascade max-breadth are correspondingly reduced. The propagation process becomes shorter, and the number of people affected decreases by orders of magnitude [Fig. 5(a)]. When the initial threshold $\theta(0)$ increases from 0.05 to 0.15 and 0.30, the percentage of propagations greater than 100 in the total number of experiments decreases from 45% to 9% and 0 [Fig. 5(d)].

Scale-Free Networks: According to Fig. 5(a)–(c), under the same conditions, the confidence intervals of scale-free networks are large compared to the confidence intervals of small-world and random networks. Fig. 5(b) shows that when the initial threshold increases from 0.05 to 0.30, the confidence interval increases significantly, and the uncertainty increases. Fig. 5(e) and (k) shows that when the initial threshold increases from 0.05 to 0.15, it has little influence on the size and
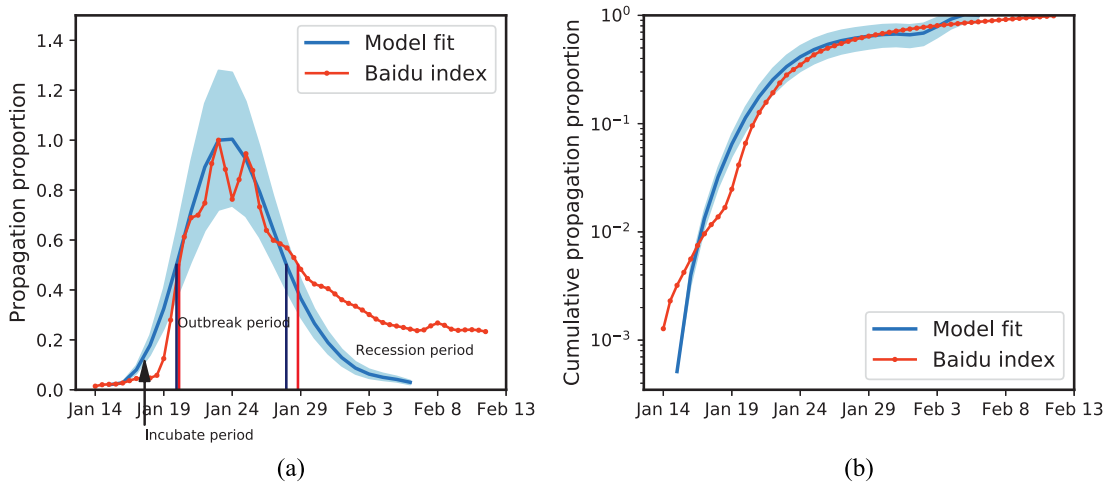
Fig. 6. Whole spreading process for online information on the topic of COVID-19 caused by the Wuhan travel ban. The red line represents Baidu index data. The blue line represents the results (average) from using the RLT model to simulate this propagation process, while the shaded areas represent the 95% confidence interval. (a) Daily propagation proportion (The denominator is the highest daily spreading number in average results.). (b) Cumulative propagation proportion (The denominator is the total diffusion numbers.).

max-breadth of the cascade; when it increases from 0.15 to 0.30, the size and max-breadth of the cascade decrease significantly. The cascade depth of propagation decreases with an increasing initial threshold [Fig. 5(h)].

Random Networks: According to Fig. 5(c), (f), (i), and (l), the effect of the initial threshold on random networks is similar to that of small-world networks. However, on the whole, with the increase in the initial threshold $\theta(0)$, the range of variation in the propagation characteristics of the random network is smaller than that of the small-world network.

IV. CASE STUDY

A. *Dissemination of Online Information About COVID-19*

Background: COVID-19 was discovered from Wuhan viral pneumonia cases in December 2019 and spread rapidly from Wuhan to almost all provinces in China. Internationally, as of April 12nd, 2020, there were more than 1 441 128 cases detected and confirmed in 184 countries. The outbreak of COVID-19 is a serious global threat [47], [48], and the online media has become the main source of public access to information about it. Public opinions and news topics related to COVID-19 have attracted continuous attention on the Internet [49].

Data Collection: In this case, we study the outbreak of online public opinion on the topic of COVID-19 caused by the Wuhan travel ban (January 23rd, 2020) in China. The data come from the Baidu index (http://index.baidu.com/). As China's largest search engine, the Baidu index reflects the spread of the incident among Chinese netizens. Since there was no official name during the initial outbreak of COVID-19, our data are derived from the sum of the Baidu index for the two keywords: 1) "Wuhan Pneumonia" and 2) "Novel Coronavirus Pneumonia."

Model Parameter Setting: The scale-free network G_4 is used in this experiment, $\theta(0) = 0.15$ and $r = 0.08$. Since the propagation of this information is explosive, samples with more than

ten propagation layers were selected from the 5000 simulation results for statistical analysis.

Results: The whole infection process for information spread is divided into three stages: 1) the incubation; 2) outbreak; and 3) recession periods. Fig. 6 compares the spreading process of online information on the topic of COVID-19 caused by the Wuhan travel ban between the actual Baidu data and the model simulation. Fig. 6(a) shows the daily spreading intensity of the information, where each layer in the RLT model represents two days. Fig. 6(b) shows the cumulative spreading intensity.

First, we combined the actual data [red line in Fig. 6(a)] to analyze the influence of psychological factors on the spreading trend. During the 7-day incubation period, the propagation growth rate was slow in the first few days and started to increase rapidly on the fifth day. Starting on January 19th, suggestions and rumors about the implementation of the Wuhan travel ban began to appear on the Internet. Due to the dissemination of this type of information, the majority of the public was in shock brought by the crisis event; when the public is in great need for information to fill the gap between their anxiety and the lack of information, they are likely to be susceptible to any information, and most people are very interested in related information. At five to seven days, the infectious spread of rumor developed aggressively. During the outbreak period, the public was eager to know the latest developments in COVID-19, and everyone talked about it and spread what they had heard. On January 23rd, due to the official implementation of the Wuhan travel ban, the spread reached its peak. During the recession period, the scope of the information spread became increasingly widespread, people gradually adapted to this kind of news, and their emotions progressively calmed down. As the event evolved over time, the public took a series of measures to address the issues and diverted part of their attention. The demand for related information continued to decline, and the public gradually lost interest. Fig. 7 shows the statistical characteristics of the cascade in model fitting.
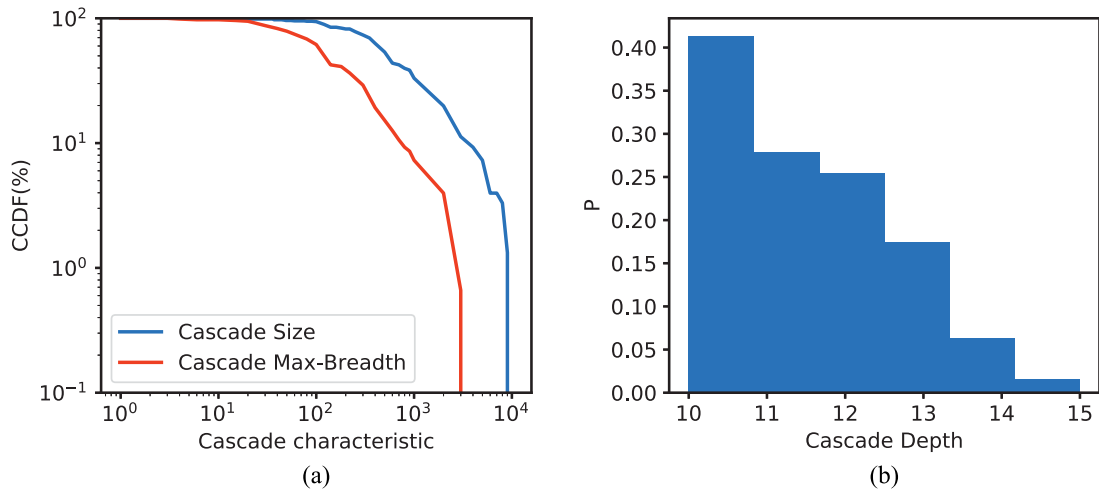
Fig. 7. Statistical characteristics of cascade in model fitting. (a) CCDFs of the size and max-breadth of diffusion cascades. (b) Histogram of the frequency distribution of cascade depth.

Analysis: Comparing the simulation results of the RLT model with the actual propagation situation (Fig. 6), we found that the model can capture the peak period of the public opinion outbreak well. The model can also well predict the start time of the outbreak period and the recession period. The prediction of the outbreak period is approximately 0.19 days earlier than the actual data, and that of the recession period is approximately 0.85 days earlier than the actual data. In addition, during the recession period, the predicted value of the model as a whole is less than the real value.

B. Dissemination of Piece of News Related to the Second Epidemic on Weibo

Background: A few months after the COVID-19 epidemic in China was brought under control, it was reported on June 11st that a local case was confirmed in Beijing, the capital of China. This news aroused people's attention and was widely spread.

Data Collection: Weibo is currently a mainstream social media with a large number of users. Many official media release news on this platform. Ordinary users can interact by reposting, commenting, and liking. We consider the news about the "Beijing Second Epidemic" published by People's Daily as an example. We collected the number of reposts of this news at various times of the day and the total number of participants. As of July 5th, 13 651 people had participated in the discussion of this news; a total of 1853 reposts, and 71.45% of the reposts were concentrated from 16:27–20:07 on June 11st. In the experiment, we only considered the spread during this time on June 11st.

Model Parameter Setting: A scale-free network with 13 651 nodes is used in this experiment, $\theta(0) = 0.05$ and $r = 0.08$. Since the People's Daily is an official account with many fans, the initial node of our experiment is randomly selected from among those nodes in the top 10% for degree. The simulation experiment was repeated 2000 times.

Results: Fig. 8 compares the spreading process for the news about the "Beijing Second Epidemic" published by the
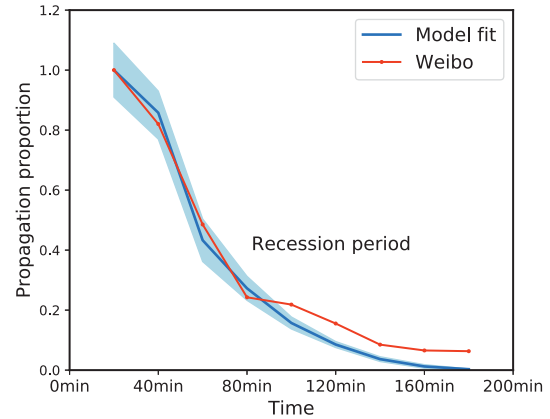

Fig. 8. Propagation process every 20 min.

People's Daily between the actual Weibo data and the model simulation. The red line in Fig. 8 shows the number of new forwardings every 20 min and indicates the spreading intensity of the information for each time period. In Fig. 8, each layer in the RLT model represents 20 min. We take the peak moment as the starting point and compare it with the model simulation results. This news on Weibo has the highest number of reposts in the first 20 min after its release, and the number of forwardings in the first 60 min accounted for 71.75% of the total that day.

Analysis: As shown in Fig. 8, the RLT model can well describe the changes in the news recession period. As the public has certain preknowledge and vigilance about COVID-19-related information, such news broke out immediately after it was released. In other words, due to the particularity of this news, there is no incubation period before spread, and the RLT model is unable accurately predict the burst characteristics of news given strong preknowledge and an emotional orientation. However, during the recession period, people's psychology and behavior are similar to the basic ideal of our model, and the RLT model can capture the gradual decline in news intensity well and predict the spreading changes in the recession period.

V. Conclusion

This article proposes a novel RLT model that is based on the attention attenuation theory and interference theory from psychology. A dynamic analysis is conducted to study the effect of network structure, the model parameter growth rate r, and the initial threshold on propagation characteristics. The case studies of the spread of COVID-19 information online were applied to prove the effectiveness of the model. Based on the above results, the following conclusions were drawn.

1) The information dissemination simulation results, which are based on the RLT model, are in some respects consistent with the characteristics of the spread of true and false news in Vosoughi *et al.*'s [41] empirical research based on Twitter data. Thus, this model can explain the propagation law of true and false news to a certain extent. We found that the features of the true news are more similar to the propagation characteristics of a simulation based on small-world networks, and that of false news is more similar to the characteristics of scale-free networks. Some statistical propagation characteristics of real social networks are closer to a mixture of small-world networks and scale-free networks. Based on this conclusion, combined with the previous research [50], we speculate that the real social network is a mixture of small-world networks and scale-free networks.

2) The network structure has a significant impact on the propagation characteristics. Information spreads most persistently in small-world networks, which decelerate and lengthen the spreading process. Information is transmitted the most rapidly in scale-free networks, and the transmission efficiency is the highest. In scale-free networks, the information transmission characteristics are not sensitive to changes in the clustering coefficient. In small-world networks, when the clustering coefficient increases, the information transmission will last longer.

3) The above conclusion remains tenable when r changes. With the increase in the growth rate r, the information transmission in small-world networks is evenly restrained. In scale-free networks, there is almost no influence on the early propagation, and the later mutation accelerates the end of the propagation. In general, in the three types of networks, with the increase in r, the total scale of transmission is significantly reduced. As r increases, the probability of explosive transmission will decrease.

4) With the increase in the initial threshold $\theta(0)$, the propagation is restrained to a certain extent, and different suppression effects are reflected in different network structures. In scale-free networks, with the increase in the initial threshold $\theta(0)$, the process of information transmission becomes shorter, the uncertainty of transmission increases, and the information has a certain probability of reaching more users. In small-world networks, with the rise in the initial threshold $\theta(0)$, the propagation process is shorter, and fewer users are affected by the information. The propagation characteristics are relatively uniform and stable with the change in the initial threshold $\theta(0)$.

By analyzing the propagation characteristics and rules of information in different networks, we can not only understand people's social behavior from the perspective of sociology but also provide the theoretical basis for public decision making, public opinion orientation, information distribution strategy, and so on. At the same time, this understanding can promote the development of political, economic, and cultural activities, offering important social significance and application value. The dissemination process for information in a network is restricted by many factors and highly complex. The spread of different types of information on diverse social platforms and among different groups of people shows great differences. By adjusting the model parameters, the RLT model can be adapted to solve various practical problems. For example, in terms of rumor control, the growth rate r can represent the ability of a rumor to incite interest, and the initial threshold $\theta(0)$ can represent the population's resistance to rumors. Andrew's latest research [51] shows that people over the age of 65 are the mainstay for forwarding fake news, and their share of forwarded false news is nearly seven times that of young and middle-aged people. Based on this conclusion, the node with a high $\theta(0)$ value can represent the knowledgeable young and middle-aged users who are immune to rumors. In contrast, a node with a low $\theta(0)$ value can represent the elderly, who are more susceptible to rumors. In terms of a network information delivery strategy, risk assessment can be carried out by combining the relationship network characteristics of different social platforms. In social networks with small-world traits, the low uncertainty of information transmission means that the risk of information release is also relatively low, and the result of release is highly predictable. In social networks with scale-free characteristics, information delivery is highly uncertain and highly risky, but with some probability, it will spread to more people at a faster rate. In terms of public opinion control, the parameter r in the model can represent the decline and interference of public attention. Inspired by the experimental conclusion that changes in r can to a large extent determine the final scale of dissemination, we can release similar novel news to reduce public attention and prevent an outbreak of public opinion. The research shows that the model proposed in this article can explain the information dissemination mechanism, explore the characteristics and laws of users on the Internet, and promote progress in this field.

It is expected that future research can optimize the model and realize the accurate prediction of information dissemination trends, prevent rumor diffusion, and control the outbreak of public opinion. The propagation characteristics and time-related dynamic propagation characteristics of the model in large empirical networks will be further investigated. The network characteristics of different social platforms will be reversely inferred through the propagation characteristics to further explore the hidden laws in network information.

REFERENCES

[1] Y. Jiang and J. C. Jiang, "Diffusion in social networks: A multiagent perspective," *IEEE Trans. Syst., Man, Cybern., Syst.*, vol. 45, no. 2, pp. 198–213, Feb. 2015.

[2] D. Davis, G. Figueroa, and Y.-S. Chen, "SociRank: Identifying and ranking prevalent news topics using social media factors," *IEEE Trans. Syst., Man, Cybern., Syst.*, vol. 47, no. 6, pp. 979–994, Jun. 2017.

[3] H. Allcott and M. Gentzkow, "Social media and fake news in the 2016 election," *J. Econ. Perspectives*, vol. 31, no. 2, pp. 211–236, 2017.

[4] M. A. Beam, M. J. Hutchens, and J. D. Hmielowski, "Facebook news and (de)polarization: Reinforcing spirals in the 2016 U.S. election," *Inf. Commun. Soc.*, vol. 21, no. 4, pp. 1–19, 2018.

[5] D. Kreiss and S. C. McGregor, "Technology firms shape political communication: The work of Microsoft, Facebook, Twitter, and Google with campaigns during the 2016 U.S. presidential cycle," *Political Commun.*, vol. 35, no. 2, pp. 155–177, 2018.

[6] Y. Gorodnichenko, T. Pham, and O. Talavera, "Social media, sentiment and public opinions: Evidence from #brexit and #uselection," Working Paper 24631, Nat. Bureau Econ. Res., Cambridge, MA, USA, 2018.

[7] M. Grcar, D. Cherepnalkoski, I. Mozetic, and P. K. Novak, "Stance and influence of Twitter users regarding the brexit referendum. comput," *Soc. Netw*, vol. 4, p. 6, Jul. 2017.

[8] P. N. Howard and B. Kollanyi, "Bots,# strongerin, and# brexit: Computational propaganda during the U.K.-EU referendum," in *Proc. SSRN*, 2016, Art. no. 2798311.

[9] E. Westlake, "Editorial comment: Post-fact performance," *Theatre J.*, vol. 70, no. 4, pp. 9–11, 2018.

[10] M. Granovetter, "Threshold models of collective behavior," *Amer. J. Sociol.*, vol. 83, no. 6, pp. 1420–1443, 1978.

[11] D. Kempe, J. Kleinberg, and É. Tardos, "Maximizing the spread of influence through a social network," in *Proc. 9th ACM SIGKDD Int. Conf. Knowl. Disc. Data Min.*, 2003, pp. 137–146.

[12] A. Goyal, W. Lu, and L. V. Lakshmanan, "Simpath: An efficient algorithm for influence maximization under the linear threshold model," in *Proc. IEEE 11th Int. Conf. Data Min.*, 2011, pp. 211–220.

[13] D. Gruhl, R. Guha, D. Liben-Nowell, and A. Tomkins, "Information diffusion through blogspace," in *Proc. 13th Int. Conf. World Wide Web*, 2004, pp. 491–501.

[14] J. Goldenberg and L. E. Muller, "Talk of the network: A complex systems look at the underlying process of word-of-mouth," *Marketing Lett.*, vol. 12, no. 3, pp. 211–223, 2001.

[15] R. Pastor-Satorras and A. Vespignani, "Epidemic spreading in scale-free networks," *Phys. Rev. Lett.*, vol. 86, no. 14, pp. 3200–3203, 2008.

[16] W. O. Kermack and A. G. McKendrick, "A contribution to the mathematical theory of epidemics," *Proc. Roy. Soc. London A Math. Phys. Character*, vol. 115, no. 772, pp. 700–721, 1927.

[17] D. H. Zanette, "Critical behavior of propagation on small-world networks," *Phys. Rev. E, Stat. Phys. Plasmas Fluids Relat. Interdiscip. Top.*, vol. 64, no. 5, 2001, Art. no. 050901.

[18] D. H. Zanette, "Dynamics of rumor propagation on small-world networks," *Phys. Rev. E, Stat. Phys. Plasmas Fluids Relat. Interdiscip. Top.*, vol. 65, no. 1, 2001, Art. no. 041908.

[19] M. Nekovee, Y. Moreno, G. Bianconi, and M. Marsili, "Theory of rumour spreading in complex social networks," *Physica A Stat. Mech. Appl.*, vol. 374, no. 1, pp. 457–470, 2008.

[20] Z. Pan, X. Wang, and X. Li, "Simulation research on rumor propagation on variable scaled networks with unscaled networks," *J. Syst. Simulat.*, vol 08, pp. 2346–2348, 2006.

[21] I. Jos-Luis and M. Esteban, "Impact of human activity patterns on the dynamics of information diffusion," *Phys. Rev. Lett.*, vol. 103, no. 3, 2009, Art. no. 038702.

[22] J. L. Iribarren and E. Moro, "Branching dynamics of viral information spreading," *Phys. Rev. E, Stat. Phys. Plasmas Fluids Relat. Interdiscip. Top.*, vol. 84, no. 4, 2011, Art. no. 046116.

[23] C. Castellano, S. Fortunato, and V. Loreto, "Statistical physics of social dynamics," *Rev. Mod. Phys.*, vol. 81, no. 2, p. 591, 2009.

[24] L.-L. Xia, G.-P. Jiang, B. Song, and Y.-R. Song, "Rumor spreading model considering hesitating mechanism in complex social networks," *Physica A Stat. Mech. Appl.*, vol. 437, pp. 295–303, Nov. 2015.

[25] Q. Liu, T. Li, and M. Sun, "The analysis of an SEIR rumor propagation model on heterogeneous network," *Physica A Stat. Mech. Appl.*, vol. 469, pp. 372–380, Mar. 2017.

[26] L. Zhao, J. Wang, Y. Chen, Q. Wang, J. Cheng, and H. Cui, "SIHR rumor spreading model in social networks," *Physica A Stat. Mech. Appl.*, vol. 391, no. 7, pp. 2444–2453, 2012.

[27] L. Zhao, X. Qiu, X. Wang, and J. Wang, "Rumor spreading model considering forgetting and remembering mechanisms in inhomogeneous networks," *Physica A Stat. Mech. Appl.*, vol. 392, no. 4, pp. 987–994, 2013.

[28] Y. Xiao, D. Chen, S. Wei, Q. Li, H. Wang, and M. Xu, "Rumor propagation dynamic model based on evolutionary game and anti-rumor," *Nonlinear Dyn.*, vol. 95, no. 1, pp. 523–539, Jan. 2019.

[29] Y. Xiao, C. Song, and Y. Liu, "Social hotspot propagation dynamics model based on multidimensional attributes and evolutionary games," *Commun. Nonlinear Sci. Numer. Simulat.*, vol. 67, pp. 13–25, Feb. 2019.

[30] Q. Li, C. Song, B. Wu, Y. Xiao, and B. Wang, "Social hotspot propagation dynamics model based on heterogeneous mean field and evolutionary games," *Physica A Stat. Mech. Appl.*, vol. 508, pp. 324–341, Oct. 2018.

[31] Y. Xiao, Q. Yang, C. Sang, and Y. Liu, "Rumor diffusion model based on representation learning and anti-rumor," *IEEE Trans. Netw. Service Manag.*, vol. 17, no. 3, pp. 1910–1923, Sep. 2013.

[32] X. He, G. Song, W. Chen, and Q. Jiang, "Influence blocking maximization in social networks under the competitive linear threshold model," in *Proc. SIAM Int. Conf. Data Min.*, 2012, pp. 463–474.

[33] K. Saito, M. Kimura, K. Ohara, and H. Motoda, "Behavioral analyses of information diffusion models by observed data of social network," in *Proc. Int. Conf. Soc. Comput. Behav. Model. Prediction*, 2010, pp. 149–158.

[34] L. Yang, Z. Li, and A. Giua, "Containment of rumor spread in complex social networks," *Inf. Sci.*, vol. 506, pp. 113–130, Jan. 2020.

[35] K. Saito, M. Kimura, K. Ohara, and H. Motoda, "Learning continuous-time information diffusion model for social behavioral data analysis," in *Proc. Adv. Mach. Learn. 1st Asian Conf. Mach. Learn. (ACML)*, Nanjing, China, Nov. 2009, pp. 322–337.

[36] J. Yang and S. Counts, "Predicting the speed, scale, and range of information diffusion in Twitter," in *Proc. 4th Int. AAAI Conf. Weblogs Soc. Media*, 2010, pp. 355–358.

[37] S. Goel, D. J. Watts, and D. G. Goldstein, "The structure of online diffusion networks," in *Proc. 13th ACM Conf. Electron. Commerce*, 2012, pp. 623–638.

[38] J. Leskovec, L. Backstrom, and J. Kleinberg, "MEME-tracking and the dynamics of the news cycle," in *Proc. 15th ACM SIGKDD Int. Conf. Knowl. Disc. Data Min.*, 2009, pp. 497–506.

[39] J. Leskovec and E. Horvitz, "Planetary-scale views on a large instant-messaging network," in *Proc. ACM 17th Int. Conf. World Wide Web*, 2008, pp. 915–924.

[40] H. Zhang, Y. Liu, and X. Chen, "Research on the information dissemination mechanisms of weibo in scale-free networks," *Physica A Stat. Mech. Appl.*, vol. 532, Oct. 2019, Art. no. 121877.

[41] S. Vosoughi, D. Roy, and S. Aral, "The spread of true and false news online," *Science*, vol. 359, no. 6380, pp. 1146–1151, 2018.

[42] P. Ozturk, H. Li, and Y. Sakamoto, "Combating rumor spread on social media: The effectiveness of refutation and warning," in *Proc. 48th Hawaii Int. Conf. Syst. Sci.*, 2015, pp. 2406–2414.

[43] D. J. Watts and S. H. Strogatz, "Collective dynamics of 'small-world' networks," *Nature*, vol. 393, no. 6684, p. 440, 1998.

[44] A.-L. Barabási and R. Albert, "Emergence of scaling in random networks," *Science*, vol. 286, no. 5439, pp. 509–512, 1999.

[45] P. Holme and B. J. Kim, "Growing scale-free networks with tunable clustering," *Phys. Rev. E, Stat. Phys. Plasmas Fluids Relat. Interdiscip. Top.*, vol. 65, no. 2, 2002, Art. no. 026107.

[46] E. N. Gilbert, "Random graphs," *Ann. Math. Stat.*, vol. 30, no. 4, pp. 1141–1144, 1959.

[47] *Coronavirus Disease 2019 (COVID-19): Situation Report, 72*, World Health Org., Geneva, Switzerland, 2020.

[48] C. Sohrabi *et al.*, "World health organization declares global emergency: A review of the 2019 novel coronavirus (COVID-19)," *Int. J. Surg.*, vol. 76, pp. 71–76, Apr. 2020.

[49] X. Han, J. Wang, M. Zhang, and X. Wang, "Using social media to mine and analyze public opinion related to COVID-19 in China," *Int. J. Environ. Res. Public Health*, vol. 17, no. 8, p. 2788, 2020.

[50] A. Sallaberry, F. Zaidi, and G. Melancon, "Model for generating artificial social networks having community structures with small world and scale free properties," *Soc. Netw. Anal. Min.*, vol. 3, no. 3, pp. 597–609, 2013.

[51] A. Guess, J. Nagler, and J. Tucker, "Less than you think: Prevalence and predictors of fake news dissemination on Facebook," *Sci. Adv.*, vol. 5, no. 1, 2019, Art. no. eaau4586.

Tianyi Luo received the B.E. degree in automation from Beijing University of Chemical Technology, Beijing, China, in 2017. She is currently pursuing the Ph.D. degree with the Institute of Automation, Chinese Academy of Sciences, Beijing. She is also with University of Chinese Academy of Sciences, Beijing, China.

Her research interests include information diffusion modeling, complex networks, social computing, and public health.

Daniel Zeng (Fellow, IEEE) received the B.S. degree in economics and operations research from the University of Science and Technology of China, Hefei, China, and the M.S. and Ph.D. degrees in industrial administration from Carnegie Mellon University, Pittsburgh, PA, USA, in 1990, 1994, and 1998, respectively.

He is Gentile Family Professor with the Department of Management Information Systems, University of Arizona, Tucson, AZ, USA. He also holds a Research Fellow position with the Institute of Automation, Chinese Academy of Sciences, Beijing, China. He has published more than 300 peer-reviewed articles. His research interests include intelligence and security informatics, infectious disease informatics, social computing, recommender systems, software agents, and applied operations research and game theory.

Dr. Zeng currently serves as the Editor in Chief of *ACM Transactions on Management Information Systems*, and the President of the IEEE Intelligent Transportation Systems Society.

Zhidong Cao received the Ph.D. degree in geographic information science from the Institute of Geographic Sciences and Nature Resources Research, Chinese Academy of Sciences, Beijing, China, in 2008.

He is currently an Associate Professor with the Institute of Automation, Chinese Academy of Sciences. His current research interests include social computing, public health, emergency management, and spatial analysis.

Qingpeng Zhang (Member, IEEE) received the B.S. degree in automation from the Huazhong University of Science and Technology, Wuhan, China, in 2009, and the Ph.D. degree in systems and industrial engineering from the University of Arizona, Tucson, AZ, USA, in 2012.

He was a Postdoctoral Research Associate with the Department of Computer Science, Tetherless World Constellation, Rensselaer Polytechnic Institute, Troy, NY, USA. He is currently an Assistant Professor with the School of Data Science, City University of Hong Kong, Hong Kong. His current research interests include social computing, complex networks, data mining, and semantic Web.

Dr. Zhang is an Associate Editor of the IEEE TRANSACTIONS ON COMPUTATIONAL SOCIAL SYSTEMS and IEEE TRANSACTIONS ON INTELLIGENT TRANSPORTATION SYSTEMS.